ISSN 0915-633X

NATIONAL INSTITUTE FOR FUSION SCIENCE

Recombining Processes in a Cooling Plasma by Mixing of Initially Heated Gas

U. Furukane, K. Sato, K. Takiyama and T. Oda

(Received – Dec. 26, 1991)

NIFS-142 Mar. 1992

RESEARCH REPORT
NIFS Series

NAGOYA, JAPAN

Recombining Processes in a Cooling Plasma by Mixing of Initially Heated Gas

Utaro Furukane, Kuninori Sato[1], Ken Takiyama[2] and Toshiatsu Oda[2]

Department of Physics, College of General Education, Ehime University, Matsuyama 790

[1]National Institute for Fusion Science, Nagoya 461-01

[2]Department of Applied Physics and Chemistry, Faculty of Engineering, Hiroshima University, Saijio, Higashi-Hiroshima 724

A numerical investigation of recombining process in a high temperature plasma in a quasi-steady state is made in a gas contact cooling, in which the initial temperature effect of contact gas heated up by the hot plasma is considered as well as the gas cooling due to the surrounding neutral particles freely coming into the plasma. The calculation has shown that the electron temperature relaxes in accord with experimental results and that the occurrence of recombining region and the inverted populations almost agree with the experimental ones.

KEYWORDS: population inversion, laser oscillation,
recombining hydrogen plasma

§1. Introduction

It has been shown that cooling plasma by contact with cold gas has a high potentiality to produce a strong nonequilibrium recombining plasma as a medium for short-wavelength laser.[1-6] One of the remarkable aspects of this scheme is that steady-state VUV laser is possible. Several experiments have been so far performed of steady-state population inversion in a plasma column (TPD-I machine).[1-3] Numerical analyses using a collisional-radiative (CR) model have also been made to clarify the atomic processes in the creation of the population inversion.[4-6]

There has been found, however, one discrepancy between the numerical analysis and experimental results that the population inversions shown in the numerical analysis take place much more rapidly than that in the experiments. One of the expected reasons is that the gas temperature at an orifice (where the steadily flowing plasma starts to contact with the introduced gas) is assumed to be as low as that of the gas surrounding the plasma column (0.05 eV). In the TPD-I machine the arc plasma produced between the cathode and anode steadily flows out through the orifice with diameter of 2 cm into a long chamber where the hydrogen molecular gas is filled for the plasma cooling and an axial magnetic field (several kG) is applied to maintain the plasma column. Then the gas temperature at the orifice is inferred to be as high as the ion temperature in the plasma because the neutral-gas density in the plasma column is lower than that of the plasma and the gas at the orifice is steadily heated

up by the collision with the ions in the steady-state plasma.

In the gas cooling experiment of the plasma in the TPD-I machine, the collisional mean free paths of the hydrogen gas particles as the cooling gas are large in comparison with diameter of the plasma column, but the particles collide each other in a distance between the orifice and the position where the population inversions are realized in the plasma column. The hot neutral gas may mainly be cooled down by the cold neutral particles coming freely from the surround gas into the plasma column as the plasma flows down along the magnetic lines of force. However, the high temperature of the neutral gas at the orifice and the cooling down of the temperature due to the cold neutral particles have not been considered although it plays an important role for the plasma cooling.[4-6]

The purpose of this paper is to numerically clarify the processes which cool the initial high temperature of the gas slowly due to the cold neutral particles. An appropriate phenomenological terms are introduced in the energy balance equation of the neutral particle for including the thermal energy reduction by the cold neutral particles, which will be estimated by using a particle kinetic model. And it is shown numerically that the cooling down of the high temperature plasma is delayed in some down stream of the plasma column, which is consistent with the experimental results.

§2. Basic Equation

The helium plasma in the TPD-I machine flows towards the down stream end of the plasma column with a constant drift velocity ($\sim 10^6$cm/s) and is confined by a constant magnetic field (B=0.4T) along the drift velocity. Under the nomal operation with hydrogen molecular gas as the contact gas, the gas with the lower density than the plasma is used as the contact gas for cooling the high-temperature helium plasma. The contact gas at the orifice is steadily heated up by the steady-state plasma flow with the flow velocity ($\sim 10^6$cm/s). Then, the gas temperature at the orifice is inferred to be as high as the ion temperature in the plasma and may be cooled down by the cold neutral particles freely coming from the surrounding as the plasma flows down along the magnetic lines of force.

In the mixing of the high temperature plasma and the hydrogen molecular gas we consider the following six dissociation processes between electron and hydrogen molecule or molecular ion:

$$e + H_2 \rightarrow H + H + e \qquad (E_1 = 8.8\text{eV}) \qquad \text{(a)}$$

$$e + H_2 \rightarrow H + H^+ + 2e \qquad (E_2 = 28.0\text{eV}) \qquad \text{(b)}$$

$$e + H_2 \rightarrow H_2^+ + 2e \qquad (E_3 = 15.42\text{eV}) \qquad \text{(c)}$$

$$e + H_2^+ \rightarrow H + H^+ + e \qquad (E_4 = 7.5\text{eV}) \qquad \text{(d)}$$

$$e + H_2^+ \rightarrow H^+ + H^+ + 2e \qquad (E_5 = 18.4\text{eV}) \qquad \text{(e)}$$

$$e + H_2^+ \rightarrow H + H \qquad (E_6 = 0.33\text{eV}) \qquad \text{(f)}$$

where the dissociated hydrogen atoms are assumed to be in the ground

state and $E_i (i = 1, \cdots, 6)$ expresses the threshold energies of each reaction. The threshold energies E_i and the reaction rates of the each dissociation processes S_i are given by Kaplan and Bengtson.[7)]

In the present calculation, the transport terms of the plasma fluid have been neglected compared with the collisional terms, and the evolution of the temperature and density of the plasma and the neutral gas have been calculated in only CR model. We consider only the region near the axis of the column and work in a coordinate system moving with the helium plasma drift velocity ($\sim 10^6$cm/s) along the plasma column.

We assume the hydrogen molecular density $n(\mathrm{H_2})$ to be constant:[4)]

$$\frac{\mathrm{d}n(\mathrm{H_2})}{\mathrm{d}t} = -n_e(S_1 + S_2 + S_3)n(\mathrm{H_2}) + \psi_0 = 0, \qquad (1)$$

where ψ_0 is the influx rate of the hydrogen molecular particle, which is balanced with the total rate of reactions (a), (b) and (c). To simplify the present calculation, it is assumed that the cooling gas flows almost together with the plasma because the plasma particles collide frequently with the gas particles. For the hydrogen molecular ion density $n(\mathrm{H_2^+})$, the excited states densities of the hydrogen atom $n_i(\mathrm{H})$ (i=2,..,20) and the hydrogen ion density $n(\mathrm{H^+})$, the corresponding equations are given by:[4)]

$$\frac{\mathrm{d}n(\mathrm{H_2^+})}{\mathrm{d}t} = n_e\mathrm{S_3}n(\mathrm{H_2}) - n_e(\mathrm{S_4} + \mathrm{S_5} + \mathrm{S_6})n(\mathrm{H_2^+}), \qquad (2)$$

$$\frac{\mathrm{d}n_i(\mathrm{H})}{\mathrm{d}t} = \sum_{j=1}^{20} a_{ij}(\mathrm{H})n_j(\mathrm{H}) + \delta_i(\mathrm{H}), \qquad (i = 2, ..., 20) \qquad (3)$$

$$\frac{\mathrm{d}n(\mathrm{H^+})}{\mathrm{d}t} = -\sum_{i=1}^{20}[\sum_{j=1}^{20} a_{ij}(\mathrm{H})n_j(\mathrm{H}) + \delta_i(\mathrm{H})] + n_e[\mathrm{S_2}n(\mathrm{H_2}) + (\mathrm{S_4} + 2\mathrm{S_5})n(\mathrm{H_2^+})], \qquad (4)$$

where the coefficients a_{ij} and δ_j are given by the radiative transition probability A_{ij} with the optical escape factor Λ_{ij}, and by the rate coefficients for the electron-impact ionization C_{ii} and recombination K_i, electron-impact excitation (C_{ij}, $i < j$) and deexcitation (C_{ji},$i < j$), and for the radiative recombination β_i.[8] The optical escape factors Λ_{1j} ($j \geq 2$) for the lines (assuming Doppler profiles for the Lyman series) are calculated simultaneously with the corresponding rate equations in the manner described in a previous paper.[9]

The corresponding equations for the helium atom densities n_i(He) (i=1,..49) and He^+ ion densities $n_i(He^+)$ (i=1,..20) are given in a similar way for the hydrogen atom.[5]

$$\frac{dn_i(\mathrm{He})}{dt} = \sum_{j=1}^{49} a_{ij}(\mathrm{He})n_j(\mathrm{He}) + \delta_i(\mathrm{He}), \qquad (i = 1, ..., 49) \qquad (5)$$

$$\frac{dn_i(\mathrm{He}^+)}{dt} = \sum_{j=1}^{20} a_{ij}(\mathrm{He}^+)n_j(\mathrm{He}^+) + \delta_i(\mathrm{He}^+). \quad (i = 1, ..., 20) \qquad (6)$$

Since the sum of the helium ion and atom density is assumed constant n_0 and the charge neutrality is assumed[4]

$$\frac{dn(\mathrm{He}^{2+})}{dt} = -\frac{dn(\mathrm{He}^+)}{dt} - \frac{dn(\mathrm{He})}{dt}, \qquad (7)$$

$$\frac{dn_e}{dt} = 2\frac{dn(\mathrm{He}^{2+})}{dt} + \frac{dn(\mathrm{He}^+)}{dt} + \frac{dn(\mathrm{H}^+)}{dt} + \frac{dn(\mathrm{H}_2^+)}{dt}, \qquad (8)$$

where n(He), $n(He^+)$ and $n(He^{2+})$ show the densities of the He atom, the He^+ ion and the He^{2+} ion, respectively.

The initial values of the population densities of the helium and hydrogen atoms and He^+ ion have been determined by solving the corresponding rate equations with the time derivatives set to be zero for the given values of the initial electron density and temperature (n_{e0} and T_{e0}).

On the axis of the TPD-I plasma column, the energy density, $3/2 \cdot n_\alpha \cdot T_\alpha$, of the atom α change with time due to the elastic and inelastic collisions with the other particles and the freely coming cold neutral particles from the surrounding of the column.

$$\frac{\mathrm{d}(\frac{3}{2} \cdot n_\alpha \cdot T_\alpha)}{\mathrm{d}t} = R_\alpha + Q_\alpha + \varepsilon_\alpha,$$

where T_α is the temperature of the atom α, R_α and Q_α denote the rate of increase of the thermal energy of the atom α due to the elastic collisions with the other particles and the inelastic collisions by the electron. To include the thermal energy reduction due to the freely coming cold neutral atoms α, the phenomenological term ε_α is introduced.

Above equation is rewritten as follows:

$$\frac{3}{2} \cdot n_\alpha \cdot \frac{\mathrm{d}}{\mathrm{d}t} T_\alpha = R_\alpha + Q_\alpha - \frac{3}{2} \cdot T_\alpha \cdot \frac{\mathrm{d}n_\alpha}{\mathrm{d}t} + \varepsilon_\alpha. \tag{9}$$

The corresponding equation for the hydrogen molecule is given by

$$\frac{3}{2} \cdot n(\mathrm{H}_2) \cdot \frac{\mathrm{d}}{\mathrm{d}t} T_m = R_m + \varepsilon_m, \tag{10}$$

where R_m and ε_m in the same meaning as R_α and ε_α for the atom α, the rate of increase of the thermal energy due to the inelastic collisions by the electron and that based on the six molecular dissociation processes are disregarded.

To simplify the calculation, The temperatures of the He and H atoms are assumed to be equal to that of the hydrogen molecule T_m as made for the ion temperatures of the previous paper,[6] that is, the temperatures of the He^{2+} and He^{+} ions are assumed in the same T_{a1}, and the temperatures T_{H+} and $T_{H_2^+}$ in T_{a2}.[6]

The following assumptions are made in the ionization and recombining processes of eq.(9)[6], that is, in the ionization processes the kinetic energy of the excited atom is transformed to that of the ion without any loss and the ionization energy is supplied by the electron, while in the recombining processes all of the corresponding energy reactions are regarded as the inverse reactions in the ionization processes. The terms Q_α and $-3/2 \cdot T_\alpha \cdot (\mathrm{d}n_\alpha/\mathrm{d}t)$ of eq.(9) for the ionizing and recombining processes are given as following. In the ionizing process such as in the reaction $\mathrm{He(j)} + \mathrm{e} \rightarrow \mathrm{He^+(1)} + 2\mathrm{e}$, since the decreasing rate of the helium atom density is $n_e \sum C_{jj}(\mathrm{He}) n_j(\mathrm{He})$,

$$Q_{\mathrm{He}} = -3/2 T_m n_e \sum C_{jj}(\mathrm{He}) n_j(\mathrm{He}),$$

and

$$-3/2 T_m \mathrm{d}n(\mathrm{He})/\mathrm{d}t = 3/2 T_m n_e \sum C_{jj}(\mathrm{He}) n_j(\mathrm{He}).$$

Then, the terms Q_{He} and $-3/2 T_m \mathrm{d}n(\mathrm{He})/\mathrm{d}t$ of eq.(9) in the ionizing process are compensated each other. Whereas, in the recombining process such as $\mathrm{He(j)} + \mathrm{e} \leftarrow \mathrm{He^+(1)} + 2\mathrm{e}$, since the increasing rate of the helium atom density is $n_e^2 n_1(\mathrm{He^+}) \sum [K_j(\mathrm{He}) + \beta_j(\mathrm{He})/n_e]$,

$$Q_{\mathrm{He}} = 3/2 T_{a1} n_e^2 n_1(\mathrm{He^+}) \sum [K_j(\mathrm{He}) + \beta_j(\mathrm{He})/n_e],$$

and

$$-3/2 T_m \mathrm{d}n(\mathrm{He})/\mathrm{d}t = -3/2 T_m n_e^2 n_1(\mathrm{He^+}) \sum [K_j(\mathrm{He}) + \beta_j(\mathrm{He})/n_e].$$

Then, in the recombination process, sum of Q_{He} and $-3/2 T_m \mathrm{d}n(\mathrm{He})/\mathrm{d}t$ of eq.(9) is given by

$$3/2 (T_{a1} - T_m) n_e^2 n_1(\mathrm{He^+}) \sum [K_j(\mathrm{He}) + \beta_j(\mathrm{He})/n_e].$$

In the reactions $H(j) + e \rightarrow H^+ + 2e$ and $H(j) + e \leftarrow H^+ + 2e$. For the ionizing process the termes Q_H and $-3/2T_m dn(H)/dt$ are compensated each other, for the recombining process the sum of these terms is expressed as follows in the same manner with the $He(j) + e \leftarrow He^+(1) + 2e$

$$Q_H - 3/2T_m dn(H)/dt = 3/2(T_{a2} - T_m)n_e^2 n_1(H^+) \sum [K_j(H) + \beta_j(H)/n_e].$$

Thus, the summation of eqs. (9) and (10) for the all species of the neutral particles result as follows:

$$\begin{aligned} \frac{dT_m}{dt} &= \sum_k \frac{1}{\tau_k}(T_e - T_m) + \sum_i \frac{1}{\tau_i}(T_{a1} - T_m) + \sum_j \frac{1}{\tau_j}(T_{a2} - T_m) \\ &+ \frac{n_e^2}{n(He) + n(H) + n(H_2)} \cdot [n(H^+)(\sum_j K_j(H) + \frac{\beta_j(H)}{n_e}) \cdot (T_{a2} - T_m) \\ &+ n_1(He^+)(\sum_j K_j(He) + \frac{\beta_j(He)}{n_e}) \cdot (T_{a1} - T_m)] + \phi. \qquad (11) \end{aligned}$$

Here K_j and β_j are the rate coefficients for the electron-impact three body recombination and the radiative recombination, respectively. τ_k (k=1,2,3) represent the collision times for (electron - He atom), (electron - H atom) and (electron - H_2 molecule), τ_i (i=1,$\cdots$,6) for (He^{2+} ion - He atom), $\cdots$ and (He^+ ion - H_2 molecule) and τ_j (j=1,$\cdots$,6) for (H^+ ion - He atom) $\cdots$ and (H_2^+ ion - H_2 molecule). The collision times for the above (electron - atom and molecule) are shown in the previous paper.[5] Those for ion - atom and molecule are approximately estimated based on the collisional cross section of $\sim 10^{-15}cm^{-2}$ and the collisional velocity of $\sim 10^6$cm/s. The last term ϕ is expressed by using ε_α and ε_m:

$$\phi = \frac{2}{3} \cdot \frac{\sum \varepsilon_\alpha + \varepsilon_m}{\sum n_\alpha + n(H_2)}.$$

The term ϕ is estimated by using a simple particle kinetic model. The thermal speed of the surrounding neutral particles and the column radius are about $\sim 10^{+5}$cm/s and $\sim$1cm, respectively. The temperature of the neutral particle in the column will be slowly cooled from the high temperature 2.5eV to the low temperature 0.05eV at $\sim 10^{-5}$s after the plasma pass through the orifice since the surrounding neutral particles pass over the column at a time interval $\sim 10^{-5}$s. Then, ϕ is estimated $\sim -2.4 \times 10^{5}$eV/s.

The equations for the electron temperature T_e, T_{a1} and T_{a2} result from the energy balance equations of the electron and the ions on the CR model as shown in Appendix.[4,6]

The ground state density n_1(H) of the hydrogen atom in the plasma region is estimated in the same way as in Ref.4,

$$n_1(\mathrm{H}) = 2 \times 10^{-18} \cdot \bar{n}_e \cdot n(\mathrm{H}_2), \qquad (12)$$

where $\bar{n}_e$ is the mean electron density over the time step which T_e cooled down until to the dissociation energy 4.48eV, and the sticking probability and the vessel volume are estimated to be 1.0 and 1.5×10^{4}cm^3 which differs from Ref.4.

The population densities of atoms and ions, the electron density, the molecular ion density and the temperatures (T_e, T_{a1}, T_{a2} and T_m) are obtained by simultaneous integration with the rate equations (1)$\sim$(6) by using equation (12) and with the differential equation (7) and (8) derived from the conservation lows and with the energy balance equations (11), (A1), (A2) and (A3) (98 equations). Integration of the equations was

performed using the high-speed Runge-Kutta method.[10)]

§3. Numerical Results and Discussion

The equations mentioned above have been integrated numerically for the initial conditions at the entrance of the plasma region in the TPD-I machine. These initial conditions are chosen as similar to the experiment performed in the machine. That is, the stationary state helium plasma whose electron density n_{e0} and temperatures T_{e0} and T_{a10} are $3.53\times10^{14}\mathrm{cm}^{-3}$ and 10eV and 5eV penetrates into a hydrogen molecular gas of 0.01 Torr. And also, the temperatures of the hydrogen ion and the neutral gases at the orifice, T_{a20} and T_{o0}, are assumed 5eV as same as T_{a10} as previously stated. Which is in contrast to the previous calculation in which the cold constant T_o(0.05eV) was assumed.[6)] The results are shown in Figs. 1 - 3.

Figure 1 shows evolutions of the temperatures T_e, T_{a1}, T_{a2} and T_o in the plasma column in which the neutral particles are almost free for incoming and outgoing to the magnetic field. As shown in the figure, the relaxation times of T_e and T_{a1} are almost the same as τ_{E}, which is about $\sim 4\times10^{-6}$s. At $\sim 4\times10^{-5}$s all the temperatures are relaxed to the order of 0.1 eV. The relaxation and relaxed time lags of T_e are about one order greater than that obtained from the previous neumerical calculation[6)] in which the neutral particles temperature is kept constant at 0.05 eV. As a result, the recombining region shown in the present

calculation appears at about 25cm downstream from the orifice and in accord with the experiment, which is noticeable in comparison with the previous analysis. And it is another important aspect shown in figure 1 that the ions and the neutral particles are cooled down with the nearly equal temperature.

The detailed description of the elastic and inelastic collisional effects on the variation of T_e, T_{a1}, T_{a2} and T_m are given in Figs. 2(a), 2(b), 2(c) and 2(d). In all Figs.2, the solid and dashed lines show the absolute values of the incoming and outgoing energy fluxes, respectively. The figures show the total energy transfer rate ($\dot{T}_e$, $\dot{T}_{a1}$, $\dot{T}_{a2}$ and $\dot{T}_m$) and the rates of the individual processes contributed to the energy transfer. The following aspects (A), (B) and (C) shown in figures are remarkable in comparison with the previous analysis:[4-6)]

(A) The heavy particle temperatures, T_{a1}, T_{a2} and T_m, do not change strongly in the early stage ($t < 2 \times 10^{-7}$s) owing to the same high initial temperature. While the electron temperature is rapidly cooled due to the molecular dissociation processes shown by the following terms in eq.(A1) (shown by 'MoL' in Fig.2a):

$$-\frac{2}{3}[\sum_{i=1}^{3} S_i E_i n(\mathrm{H}_2) + \sum_{i=4}^{6} S_i E_i n(\mathrm{H}_2^+)]$$

and

$$-T_e[\sum_{i=2}^{3} S_i n(\mathrm{H}_2) + \sum_{i=5}^{6}(-1)^{i-1} S_i n(\mathrm{H}_2^+)].$$

Then, at the time of 5×10^{-7}s the electron temperature are much more cooled down than the heavy particle ones. In the time interval from 2×10^{-7}s to 5×10^{-6}s, the effect of the electron elastic collisions with the

heavy particle, that is, $2/3\sum 1/\tau_{eh}\cdot(T_h-T_e)$ (shown by E in Fig.2a) are the incoming processes of the energy flux to the electrons (mainly with the ions), and the electron temperature increase to that of the heavy particle. Therefore, at the time of $\sim 5\times10^{-6}$s the elastic collision and dissociation processes make the electrons cool in the same rate together with the heavy particles. At $t > 5\times10^{-6}$s, as shown in Fig.2(a), the cooling rate by the inelastic collision is small and the heating rate by the deexcitation processes increase, The heating is more or less overcomed by the cooling due to the elastic collision with the neutral particles which is mainly cooled by the particles freely coming from the surrounding region. Therefore, in $t > 5\times10^{-6}$s the electron are slowly cooled and T_e decrease to $\sim$0.1eV at $\sim 1\times10^{-4}$s.

(B) In the early stage(2×10^{-7}s$< t < 5\times10^{-7}$s), the ions are cooled mainly by the collision with the electron (shown by '$E\cdot I+E$' in Figs.2b and 2c). Therefore, in the time interval from 5×10^{-7}s to 5×10^{-6}s, the effect of the elastic collisions between the neutral particle and the ions, that is, $1/\tau_{atom,He_{ion}}\cdot(T_0-T_{a1})$ in eq.(A2) (shown by '$E\cdot A$' in Fig.2b) and $1/\tau_{atom,H+}\cdot(T_0-T_{a2})$ in eq.(A3) (shown by '$E\cdot A$' in Fig.2c) [$\tau_{atom,He_{ion}}$ and $\tau_{atom,H+}$ are the collision times for (atoms-He ions) and (atoms-hydrogen ions)] are the incoming processes of the energy flux to the ions because the ion temperatures are lower than that of the neutral particles due to the strong collision between the ions and electron in the early stage (2×10^{-7}s$< t < 5\times10^{-6}$s). Then, at the time of $\sim 5\times10^{-6}$s, the cooling of the ions is caused in the same rate together with the other particle. At $t > 5\times10^{-6}$s, as shown in Figs.2(b)and 2(c), the ions are

cooled with the small rate given by the difference between the cooling rate by the ionization processes and the heating rate by the elastic collision with the electron which is cooled down to ~0.1eV at 5×10^{-5}s.

(C) As shown in Eq.(11), the inelastic energy transfer of the neutral particle is attributed to the recombining processes (shown by 'R' in Fig.2d) shown by term

$$\frac{n_e^2}{n(\mathrm{He}) + n(\mathrm{H}) + n(\mathrm{H_2})} \cdot [n(\mathrm{H^+})(\sum_j K_j(\mathrm{H}) + \frac{\beta_j(\mathrm{H})}{n_e}) \cdot (T_{a2} - T_m) + n_1(\mathrm{He^+}) \cdot (\sum_j K_j(\mathrm{He}) + \frac{\beta_j(\mathrm{He})}{n_e}) \cdot (T_{a1} - T_m)]$$

and the energy transfer rate by the processes are incoming for the higher ion temperature than the atom temperature, and are outgoing for the lower ion temperature than the atom temperature. At 5×10^{-7}s and 5×10^{-6}s, the sign of these temperature difference change consistently with the direction of the energy transfer by the recombining processes as shown in Figs.2(d). At $t > 5 \times 10^{-6}$s, as shown Fig.2(d), the neutral particles are cooled with the small rate ($< 2 \times 10^5$eV/s) given by the difference between the phenomenological thermal energy reduction ϕ and the energy incoming rate accompanied by the recombining processes.

Figure 3 shows the evolution of the over-population density $\Delta n_{32}(\mathrm{H})$. The simulation results of n_e, $n(\mathrm{He^{2+}})$, $n(\mathrm{H^+})$, $n_j(\mathrm{H})/\omega_j$ $(i = 1, 2, \cdots)$ (ω_j is statistical weight of level j) are almost same that of previous paper[6] with the exception of a delay of the recombining time and a little reduction of the population density due to this delay.

The × symbols in Figs. 1 and 3 express observed values in the TPD-I machine[1]. These observed values should be obtained at the time 3×10^{-5}s

at which $\Delta n_{32}(\mathrm{H})$ shows the maximum value. The calculated values at that time are shown in each figure by the symbol •, which is consistent with the experimental results. Then, the calculated results based on the present CR model which assume the hot gas temperature at the orifice can be used in the estimation of the inverted population of the recombining hydrogen plasma in the TPD-I machine because each calculated and observed value is not only in the same order range but also the recombining region is in accord with the experimental result.

The phenomenological thermal energy reduction term ϕ, which is the cooling rate of the neutral particle in the plasma column due to the freely coming in and out the plasma, is estimated $\sim$-2.4×10^5eV/s as previously stated. The rate is smaller than the electron temperature cooling rate based on the inelastic collision with the atomes and ions. Particularly, at $t > 5\times10^{-6}$s, the cooling of the neutral particle make to retard as shown in Fig.2(d) owing to heating up by the recombining processes. Then, the higher temperature of the neutral particle in the column continues until $\sim 3\times10^{-5}$s unlike the surrounding neutral particle.

On the other hand, at $t > 5\times10^{-6}$s the cooling of the electron temperature (down to $\sim$0.1eV) is due to the elastic collision with the neutral particle as shown in Fig.2(a). Since the neutral particle temperature in the column is kept more than 0.1eV until $\sim 3\times10^{-5}$s the electron is slowly cooled down to 0.1eV at $\sim 10^{-4}$s. It is attributed to the high temperature of the ions and the neutral particle at the orifice that the slowly cooling of the electron temperature are obtaind in the present calculation.

The present calculation is based on the one dimentional treatment

in which the constant drift velocity is assumed. And we modelled the cooling neutral gas as that it is heated by the hot plasma at the orifice and is cooled by the neutral gas particle freely coming in and out the plasma column from the surounding space. As a result, the reasonable results are obtained in comparison with the experimental ones.

§4. Conclusions

The neutral gas temperature at the orifice is infered to be as high as the ion one in the gas contact experiment with the TPD-I plasma. The steady state flow plasma with the high initial gas temperature is numerically analized by using the energy balance equation in which the energy reduction due to the neutral particles freely coming in and out the plasma are taken into account by using the phenomenological term for the neutral particles estimated on the basis of a particle-kinetic model. As a result, the calculated recombining region is close to the experimental ones as well as the calculated population densities are. Therefore, the calculated results based on the present treatment can be applied to the estimation of the inverted population of the recombining plasma in the TPD-I machine.

Appendix

The following equations for the electron temperature T_e and the ion temperatures T_{a1} and T_{a2} results from the energy balance equation of the electron and the ions on the CR model.[4,6)]

$$\begin{aligned}\frac{dT_e}{dt} &= \frac{2}{3}\sum_h \frac{1}{\tau_{eh}}(T_h - T_e) - \frac{2}{3}\sum_k \sum_{i=2}^{l}\sum_{j=1}^{i-1}(E_j - E_i)(C_{ji}n_j - C_{ij}n_i) \\ &- \frac{2}{3}\sum_k \sum_{j=1}^{l}(E_j + \frac{3}{2}T_e)C_{jj}n_j \\ &+ \frac{2}{3}n_e n_{ion}\sum_k \sum_{j=1}^{l}(E_j + \frac{3}{2}T_e)(K_j + \frac{\beta_j}{n_e}) \\ &- \frac{2}{3}\sum_{i=1}^{3} S_i E_i n(\mathrm{H}_2) - \frac{2}{3}\sum_{i=4}^{6} S_i E_i n(\mathrm{H}_2^+) \\ &- T_e[\sum_{i=2}^{3} S_i n(\mathrm{H}_2) + \sum_{i=5}^{6}(-1)^{i-1} S_i n(\mathrm{H}_2^+)], \qquad (A1)\end{aligned}$$

$$\begin{aligned}\frac{dT_{a1}}{dt} &= (\frac{1}{\tau_{e,H_e^{2+}}} + \frac{1}{\tau_{e,H_e^+}})(T_e - T_{a1}) + (\frac{1}{\tau_{H^+,H_e^{2+}}} + \frac{1}{\tau_{H^+,H_e^+}})(T_{a2} - T_{a1}) \\ &+ \frac{1}{\tau_{atom,He ion}}(T_m - T_{a1}) \\ &+ \frac{n_e}{n(\mathrm{He}^{2+}) + n(\mathrm{He}^+)}\sum_j C_{jj}(\mathrm{He})n_j(\mathrm{He})(T_m - T_{a1}), \qquad (A2)\end{aligned}$$

$$\begin{aligned}\frac{dT_{a2}}{dt} &= (\frac{1}{\tau_{e,H^+}} + \frac{1}{\tau_{e,H_2^+}})(T_e - T_{a2}) + (\frac{1}{\tau_{H_e^{2+},H^+}} + \frac{1}{\tau_{H_e^+,H^+}})(T_{a1} - T_{a2}) \\ &+ \frac{1}{\tau_{atom,H^+}}(T_m - T_{a2}) \\ &+ \frac{n_e}{n(\mathrm{H}^+) + n(\mathrm{H}_2^+)}\sum_j C_{jj}(\mathrm{H})n_j(\mathrm{H})(T_m - T_{a2}). \qquad (A3)\end{aligned}$$

Where the collision times τ_{eh} et al. are shown in refs.5 and 6. And, on the occasion of the reading of eqs.(A2) and (A3), following assumption

is used: in ionization processes, the kinetic energy of the excited atom is transformed to that of the ion without any loss, and the ionization energy is supplied by the electron, while in the recombining processes, all of the corresponding energy reactions are regarded as the inverse reactions in the ionization processes.[5,6)]

Acknowledgments

The authors would like to thank Prof. M. Otsuka of the Department of Liberal Arts, Kansai Medical University and Prof. J.Fujita of the National Institute for Fusion Science for their useful discussions. This study was carried out as a part of a collaborating research project at the National Institute for Fusion Science (formerly Institute of Plasma Physics, Nagoya University). This work was also supported in part by a Grant-in-Aid for Scientific Research from the Ministry of Education, Science and Culture. The numerical calculations have been made at the Computer Center of the National Institute for Fusion Science.

References

1) M.Otsuka: Appl.Opt. 19 (1980) 3904.

2) K.Sato, M.Shiho, M.Hosokawa, H.Sugawara, T.Oda, and T.Sasaki: Phys.Rev.Lett. 39(1977) 1074.

3) T.Oda, K.Takiyama, Y.Kamiura, T.Fujita, K.Sato, K.Ishii, R.Akiyama, M.Otsuka, U.Furukane, H.Sakai, K.Ono and T.Oomori: *Short Wave Length Lasers and Their Applications, Proc. Int.Symp., Osaka,1987*,ed.C.Yamanaka, Springer Proc. Phys. Vol.30,(1988) pp.42-49.

4) U.Furukane, K.Sato and T.Oda: Jpn J.Appl.Phys. 29 (1990) 1814.

5) U.Furukane, K.Sato and T.Oda: J.Phys. D: Appl.Phys. 22(1987) 512.

6) U.Furukane, K.Sato, K.Takiyama and T.Oda: Jpn J.Appl.Phys. 30 (1991) 1272.

7) D.J.Kaplan and R.D.Bengtson: J.Phys. B: At.Mol.Phys. 14 (1981) 1983.

8) L.C.Johnson: Astrophys.J. 174 (1972) 227.

9) U.Furukane, T.Yokota, K.Kawasaki and T.Oda: J.Quant.Spectr.Radiat. Transfer 29 (1983) 75.

10) Y.Tsuji, T.Oda, and U.Furukane: T.IEE Japan 107-A (1987) 517.

Fig. 1. Time histories of the electron temperature 'T_e', the helium ion temperature 'T_{a1}', the hydrogen ion temperature 'T_{a2}' and the neutral particle temperature 'T_o'. The marks × and • show the observed T_e and the corresponding calculated value.

Fig. 2(a). Time histories of the total electron energy transfer rate '$\dot{T}_e$', the electron energy transfer rate by all elastic collisions 'E', sum of the rate by ionization and recombination for H atom 'I + R' and the rate by excitation and deexcitation for H atom 'E + D', sum of the rates by molecular disociation processes 'Mol'.

Fig. 2(b). Time histories of the total helium ion energy transfer rate '$\dot{T}_{a1}$', the helium ions energy transfer rate by the elastic collision with the neutral particles 'E · A', sum of the rate by the elastic collisions with the electron and with the hydrogen ions 'E · I + E', and the due to the ionization by the electron 'I'.

Fig. 2(c). Time histories of the total hydrogen ion energy transfer rate '$\dot{T}_{a2}$', the hydrogen ions energy transfer rate by the elastic collision with the neutral particles 'E · A', sum of the rate by the elastic collisions with the electron and with the helium ions 'E · I + E', and the rate due to the ionization by the electron 'I'.

Fig. 2(d). Time histories of the neutral particle energy transfer rate '$\dot{T}_0$', the neutral particle energy transfer rate by the elastic collision with the all ions 'E · I', the rate by the elastic collisions with the electron 'E · E', and the rate due to the recombination by the electron 'R' and 'DIFF' show the phenomenological reduction rate.

Fig. 3. Time histories of the overpopulation densities Δn_{32}(H) of H atom (a)

in the constant low $T_0 = 0.05$eV, (b) in present calculation. The marks $\times$ and $\bullet$ show the observed Δn_{32}(H) and the corresponding calculated values.

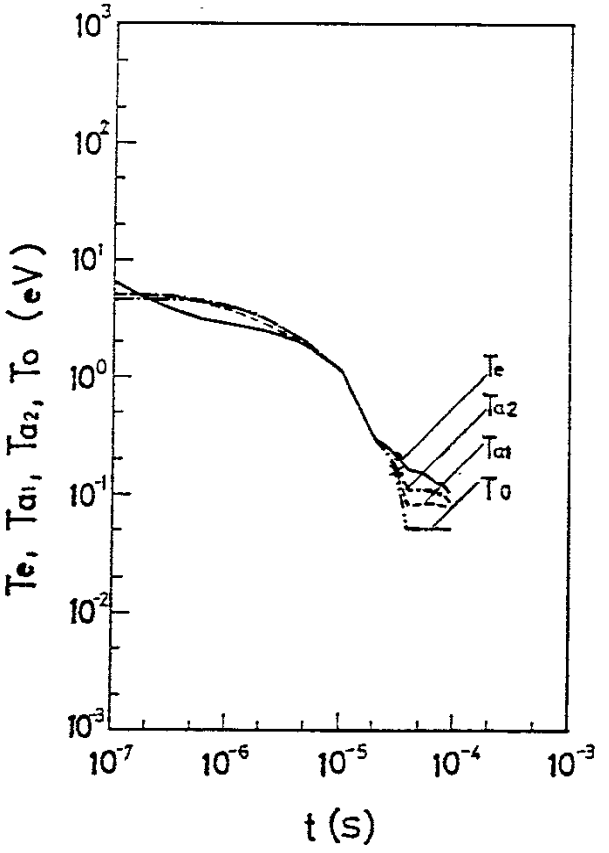
10^3
10^2
10^1
10^0
10^{-1}
10^{-2}
10^{-3}
T_e, T_{a1}, T_{a2}, T_0 (eV)
10^{-7}
10^{-6}
10^{-5}
10^{-4}
10^{-3}
t (s)
T_e
T_{a2}
T_{a1}
T_0

Fig. 1

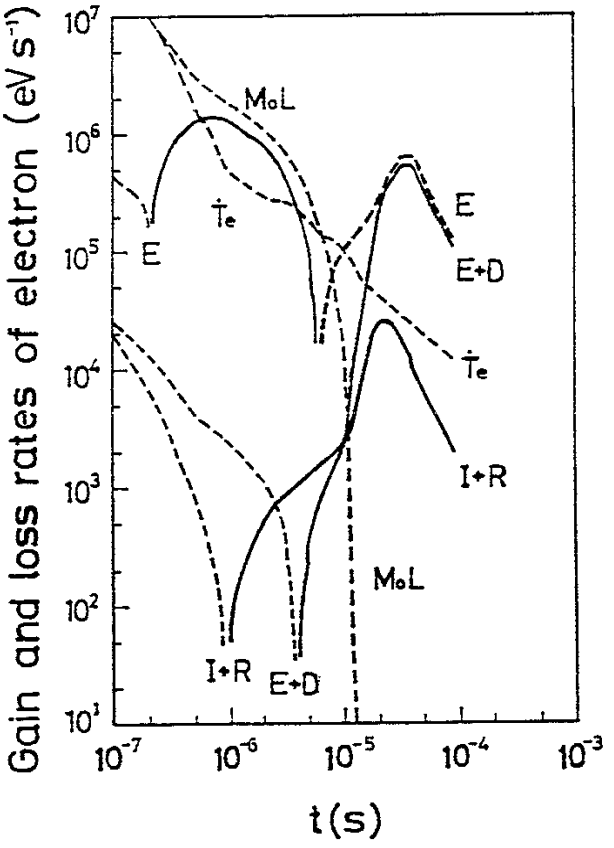
Gain and loss rates of electron (eV s⁻¹)
10⁷
10⁶
10⁵
10⁴
10³
10²
10¹
10⁻⁷
10⁻⁶
10⁻⁵
10⁻⁴
10⁻³
t(s)
MoL
Ṫe
E
E
E+D
Ṫe
I+R
MoL
I+R
E+D

Fig. 2(a)

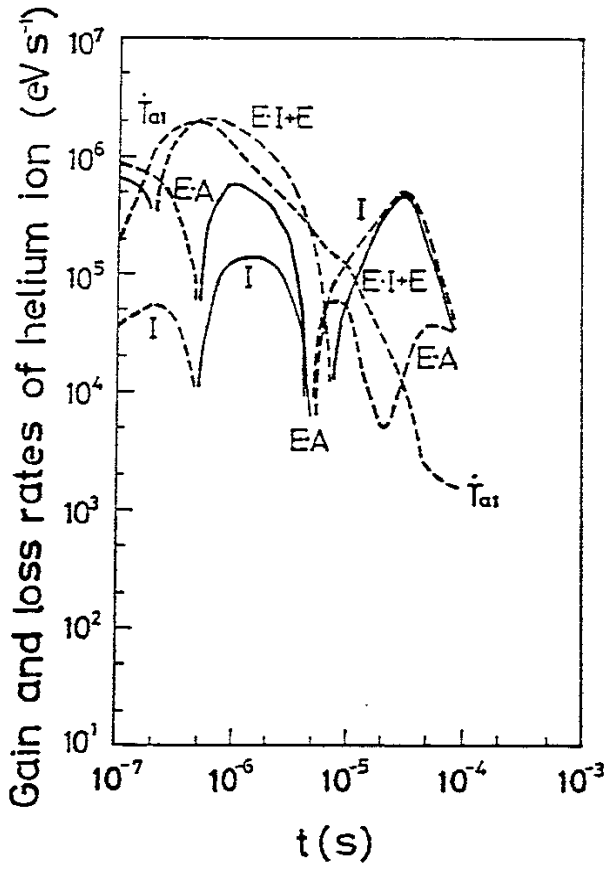
Gain and loss rates of helium ion (eV s⁻¹)
10⁷
10⁶
10⁵
10⁴
10³
10²
10¹
10⁻⁷
10⁻⁶
10⁻⁵
10⁻⁴
10⁻³
t (s)
Ṫa1
E·I+E
E·A
I
I
E·I+E
E·A
EA
Ṫa1

Fig. 2(b)

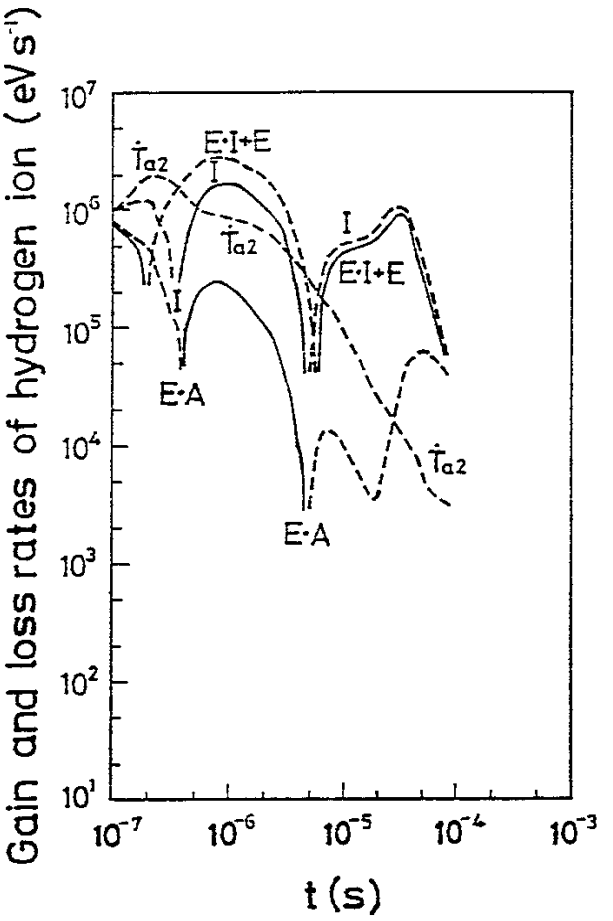
Gain and loss rates of hydrogen ion (eV s⁻¹)
10⁷
10⁶
10⁵
10⁴
10³
10²
10¹
10⁻⁷
10⁻⁶
10⁻⁵
10⁻⁴
10⁻³
t (s)
E·I+E
Ṫa2
I
E·A

Fig. 2(c)

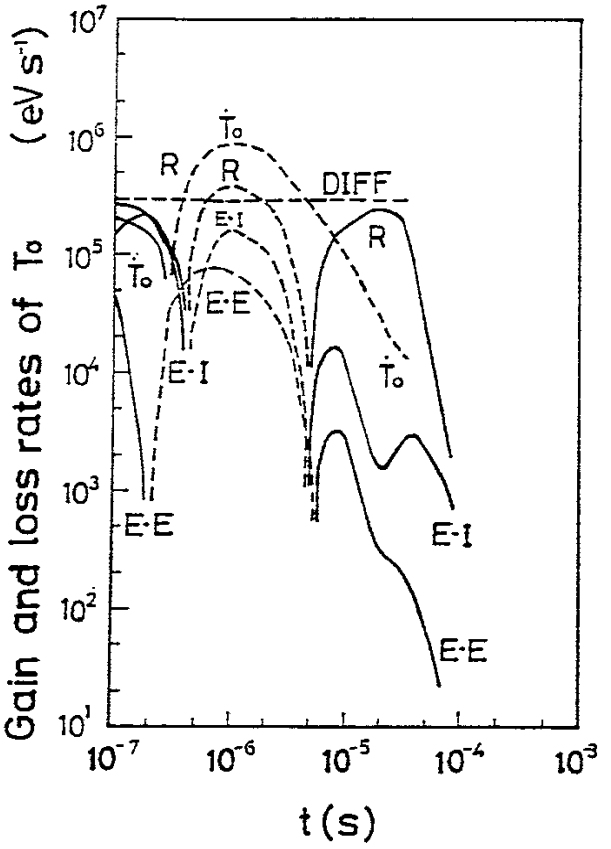
Gain and loss rates of $\dot{T}_0$ (eV s^{-1})
10^7
10^6
10^5
10^4
10^3
10^2
10^1
10^{-7}
10^{-6}
10^{-5}
10^{-4}
10^{-3}
t (s)
$\dot{T}_0$
R
R
DIFF
E-I
$\dot{T}_0$
E-E
E-I
E-E
R
$\dot{T}_0$
E-I
E-E

Fig. 2(d)

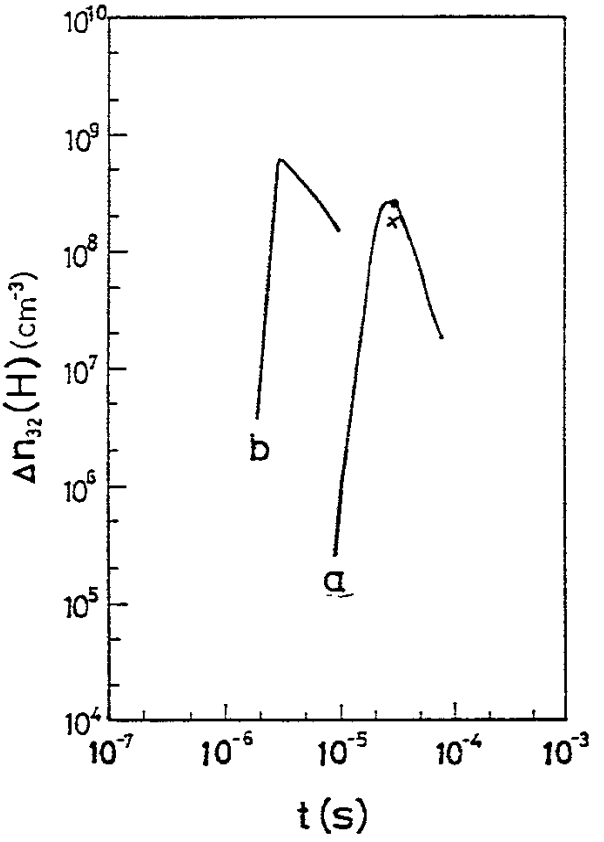
10^{10}
10^{9}
10^{8}
10^{7}
10^{6}
10^{5}
10^{4}
$\Delta n_{32}(H)\,(cm^{-3})$
b
a
x
10^{-7}
10^{-6}
10^{-5}
10^{-4}
10^{-3}
t (s)

Fig. 3

Recent Issues of NIFS Series

NIFS-91 M. Tanaka, S. Murakami, H. Takamaru and T.Sato, *Macroscale Implicit, Electromagnetic Particle Simulation of Inhomogeneous and Magnetized Plasmas in Multi-Dimensions;* May 1991

NIFS-92 S. - I. Itoh, *H-mode Physics, -Experimental Observations and Model Theories-, Lecture Notes, Spring College on Plasma Physics, May 27 - June 21 1991 at International Centre for Theoretical Physics (IAEA UNESCO) Trieste, Italy ;* Jun. 1991

NIFS-93 Y. Miura, K. Itoh, S. - I. Itoh, T. Takizuka, H. Tamai, T. Matsuda, N. Suzuki, M. Mori, H. Maeda and O. Kardaun, *Geometric Dependence of the Scaling Law on the Energy Confinement Time in H-mode Discharges;* Jun. 1991

NIFS-94 H. Sanuki, K. Itoh, K. Ida and S. - I. Itoh, *On Radial Electric Field Structure in CHS Torsatron / Heliotron;* Jun. 1991

NIFS-95 K. Itoh, H. Sanuki and S. - I. Itoh, *Influence of Fast Ion Loss on Radial Electric Field in Wendelstein VII-A Stellarator;* Jun. 1991

NIFS-96 S. - I. Itoh, K. Itoh, A. Fukuyama, *ELMy-H mode as Limit Cycle and Chaotic Oscillations in Tokamak Plasmas;* Jun. 1991

NIFS-97 K. Itoh, S. - I. Itoh, H. Sanuki, A. Fukuyama, *An H-mode-Like Bifurcation in Core Plasma of Stellarators;* Jun. 1991

NIFS-98 H. Hojo, T. Watanabe, M. Inutake, M. Ichimura and S. Miyoshi, *Axial Pressure Profile Effects on Flute Interchange Stability in the Tandem Mirror GAMMA 10;* Jun. 1991

NIFS-99 A. Usadi, A. Kageyama, K. Watanabe and T. Sato, *A Global Simulation of the Magnetosphere with a Long Tail : Southward and Northward IMF;* Jun. 1991

NIFS-100 H. Hojo, T. Ogawa and M. Kono, *Fluid Description of Ponderomotive Force Compatible with the Kinetic One in a Warm Plasma* ; July 1991

NIFS-101 H. Momota, A. Ishida, Y. Kohzaki, G. H. Miley, S. Ohi, M. Ohnishi K. Yoshikawa, K. Sato, L. C. Steinhauer, Y. Tomita and M. Tuszewski *Conceptual Design of D-^{3}He FRC Reactor "ARTEMIS"* ; July 1991

NIFS-102 N. Nakajima and M. Okamoto, *Rotations of Bulk Ions and Impurities in Non-Axisymmetric Toroidal Systems* ; July 1991

NIFS-103 A. J. Lichtenberg, K. Itoh, S. - I. Itoh and A. Fukuyama, *The Role of Stochasticity in Sawtooth Oscillation* ; Aug. 1991

NIFS-104 K. Yamazaki and T. Amano, *Plasma Transport Simulation Modeling for Helical Confinement Systems;* Aug. 1991

NIFS-105 T. Sato, T. Hayashi, K. Watanabe, R. Horiuchi, M. Tanaka, N. Sawairi and K. Kusano, *Role of Compressibility on Driven Magnetic Reconnection ;* Aug. 1991

NIFS-106 Qian Wen - Jia, Duan Yun - Bo, Wang Rong - Long and H. Narumi, *Electron Impact Excitation of Positive Ions - Partial Wave Approach in Coulomb - Eikonal Approximation* ; Sep. 1991

NIFS-107 S. Murakami and T. Sato, *Macroscale Particle Simulation of Externally Driven Magnetic Reconnection;* Sep. 1991

NIFS-108 Y. Ogawa, T. Amano, N. Nakajima, Y. Ohyabu, K. Yamazaki, S. P. Hirshman, W. I. van Rij and K. C. Shaing, *Neoclassical Transport Analysis in the Banana Regime on Large Helical Device (LHD) with the DKES Code;* Sep. 1991

NIFS-109 Y. Kondoh, *Thought Analysis on Relaxation and General Principle to Find Relaxed State;* Sep. 1991

NIFS-110 H. Yamada, K. Ida, H. Iguchi, K. Hanatani, S. Morita, O. Kaneko, H. C. Howe, S. P. Hirshman, D. K. Lee, H. Arimoto, M. Hosokawa, H. Idei, S. Kubo, K. Matsuoka, K. Nishimura, S. Okamura, Y. Takeiri, Y. Takita and C. Takahashi, *Shafranov Shift in Low-Aspect-Ratio Heliotron / Torsatron CHS* ; Sep 1991

NIFS-111 R. Horiuchi, M. Uchida and T. Sato, *Simulation Study of Stepwise Relaxation in a Spheromak Plasma ;* Oct. 1991

NIFS-112 M. Sasao, Y. Okabe, A. Fujisawa, H. Iguchi, J. Fujita, H. Yamaoka and M. Wada, *Development of Negative Heavy Ion Sources for Plasma Potential Measurement* ; Oct. 1991

NIFS-113 S. Kawata and H. Nakashima, *Tritium Content of a DT Pellet in Inertial Confinement Fusion* ; Oct. 1991

NIFS-114 M. Okamoto, N. Nakajima and H. Sugama, *Plasma Parameter Estimations for the Large Helical Device Based on the Gyro-Reduced Bohm Scaling* ; Oct. 1991

NIFS-115 Y. Okabe, *Study of Au^- Production in a Plasma-Sputter Type Negative Ion Source* ; Oct. 1991

NIFS-116 M. Sakamoto, K. N. Sato, Y. Ogawa, K. Kawahata, S. Hirokura, S. Okajima, K. Adati, Y. Hamada, S. Hidekuma, K. Ida, Y. Kawasumi, M. Kojima, K. Masai, S. Morita, H. Takahashi, Y. Taniguchi, K. Toi and T. Tsuzuki, *Fast Cooling Phenomena with Ice Pellet Injection in the JIPP T-IIU Tokamak;* Oct. 1991

NIFS-117 K. Itoh, H. Sanuki and S. -I. Itoh, *Fast Ion Loss and Radial Electric Field in Wendelstein VII-Λ Stellarator*; Oct. 1991

NIFS-118 Y. Kondoh and Y. Hosaka, *Kernel Optimum Nearly-analytical Discretization (KOND) Method Applied to Parabolic Equations <<KOND-P Scheme>>;* Nov. 1991

NIFS-119 T. Yabe and T. Ishikawa, *Two- and Three-Dimensional Simulation Code for Radiation-Hydrodynamics in ICF*; Nov. 1991

NIFS-120 S. Kawata, M. Shiromoto and T. Teramoto, *Density-Carrying Particle Method for Fluid* ; Nov. 1991

NIFS-121 T. Ishikawa, P. Y. Wang, K. Wakui and T. Yabe, *A Method for the High-speed Generation of Random Numbers with Arbitrary Distributions;* Nov. 1991

NIFS-122 K. Yamazaki, H. Kaneko, Y. Taniguchi, O. Motojima and LHD Design *Group, Status of LHD Control System Design ; Dec. 1991*

NIFS-123 Y. Kondoh, *Relaxed State of Energy in Incompressible Fluid and Incompressible MHD Fluid* ; Dec. 1991

NIFS-124 K. Ida, S. Hidekuma, M. Kojima, Y. Miura, S. Tsuji, K. Hoshino, M. Mori, N. Suzuki, T. Yamauchi and JFT-2M Group, *Edge Poloidal Rotation Profiles of H-Mode Plasmas in the JFT-2M Tokamak ;* Dec. 1991

NIFS-125 H. Sugama and M. Wakatani, *Statistical Analysis of Anomalous Transport in Resistive Interchange Turbulence* ;Dec. 1991

NIFS-126 K. Narihara, *A Steady State Tokamak Operation by Use of Magnetic Monopoles* ; Dec. 1991

NIFS-127 K. Itoh, S. -I. Itoh and A. Fukuyama, *Energy Transport in the Steady State Plasma Sustained by DC Helicity Current Drive* ;Jan. 1992

NIFS-128 Y. Hamada, Y. Kawasumi, K. Masai, H. Iguchi, A. Fujisawa, JIPP T-IIU Group and Y. Abe, *New Hight Voltage Parallel Plate Analyzer* ; Jan. 1992

NIFS-129 K. Ida and T. Kato, *Line-Emission Cross Sections for the Charge-exchange Reaction between Fully Stripped Carbon and Atomic Hydrogen in Tokamak Plasma*; Jan. 1992

NIFS-130 T. Hayashi, A. Takei and T. Sato, *Magnetic Surface Breaking in 3D MHD Equilibria of l=2 Heliotron* ; Jan. 1992

NIFS-131 K. Itoh, K. Iguchi and S. -I. Itoh, *Beta Limit of Resistive Plasma in Torsatron/Heliotron* ; Feb. 1992

NIFS-132 K. Sato and F. Miyawaki, *Formation of Presheath and Current-Free Double Layer in a Two-Electron-Temperture Plasma* ; Feb. 1992

NIFS-133 T. Maruyama and S. Kawata, *Superposed-Laser Electron Acceleration* Feb. 1992

NIFS-134 Y. Miura, F. Okano, N. Suzuki, M. Mori, K. Hoshino, H. Maeda, T. Takizuka, JFT-2M Group, S.-I. Itoh and K. Itoh, *Rapid Change of Hydrogen Neutral Energy Distribution at L/H-Transition in JFT-2M H-mode ;* Feb. 1992

NIFS-135 H. Ji, H. Toyama, A. Fujisawa, S. Shinohara and K. Miyamoto *Fluctuation and Edge Current Sustainment in a Reversed-Field-Pinch;* Feb. 1992

NIFS-136 K. Sato and F. Miyawaki, *Heat Flow of a Two-Electron-Temperature Plasma through the Sheath in the Presence of Electron Emission;* Mar. 1992

NIFS-137 T. Hayashi, U. Schwenn and E. Strumberger, *Field Line Diversion Properties of Finite ß Helias Equilibria;* Mar. 1992

NIFS-138 T. Yamagishi, *Kinetic Approach to Long Wave Length Modes in Rotating Plasmas*; Mar. 1992

NIFS-139 K. Watanabe, N. Nakajima, M. Okamoto, Y. Nakamura and M. Wakatani, *Three-dimensional MHD Equilibrium in the Presence of Bootstrap Current for Large Helical Device (LHD)*; Mar. 1992

NIFS-140 K. Itoh, S. -I. Itoh and A. Fukuyama, *Theory of Anomalous Transport in Toroidal Helical Plasmas;* Mar. 1992

NIFS-141 Y. Kondoh, *Internal Structures of Self-Organized Relaxed States and Self-Similar Decay Phase;* Mar. 1992